Response to Referee #3

This study by Zhang et al. (2026) addresses the incomplete representation of isoprene-derived secondary organic aerosol (ISOA) formation in global chemical models. The authors updated the isoprene NOx-dependent chemistry scheme that explicitly treats key reactive uptake intermediates IEPOX and HMML/MAE and their respective heterogenous reaction products in the CAM6-Chem. The updated ISOA representations were evaluated against observations showing improved speciation and better agreement with the observed organic aerosol concentrations across China. With the updated chemistry, the authors evaluated the spatial the spatial and seasonal characteristics of ISOA, revealing IEPOX products (low NOx pathway) dominate ISOA on a nation-scale while HMML/MAE products contribute much less but are more significant in NOx-rich regions of Eastern China. ISOA exhibits strong seasonal variability, peaking in summer, consistent with seasonal peaks in biogenic isoprene emissions, hydroxyl radicals (OH), and aerosol-phase heterogenous chemistry predictors (pH, sulfate, aerosol liquid water). Simulated long-term (2000–2019) trends show ISOA change were slightly negative but certain regions like SWC and SGN have contrasting changes. Regional differences in ISOA change drivers and temporal evolution of subspecies highlighted distinct controlling factors, with precursor supply being more important in SWC and sulfate-related heterogeneous reaction conditions in SGN. The authors also note limitations, such as the absence of explicit isoprene cloud-water chemistry in CAM6-Chem, suggesting areas for future model refinement and the need for more composition-resolved observations Overall, this study fills a critical gap by integrating both IEPOX and MAE/HMML pathways into global models. This enables more robust evaluation of the long-term trend of ISOA, providing new insights into the key drivers of regional heterogeneity and directly inform regional air quality. The science is carefully executed and presented. The manuscript suitable for ACP after addressing the comments below.

We are very grateful to the reviewer for the constructive evaluation and helpful suggestions, which have allowed us to clarify and improve the manuscript. Before addressing the reviewer's comments point by point, we briefly summarize the major revisions made in response to Referee #3. The reviewer's comments are shown in **bold blue text**, while our responses and the corresponding revised manuscript text are shown in black text. Line numbers refer to the revised manuscript.

In response to Referee #3, we substantially revised the model description and implementation of epoxide-derived ISOA formation. Most importantly, we replaced the initially submitted parallel-sink treatment with a relative-rate branching framework, in which total epoxide uptake is first calculated using $k_{aq,total}$ and then partitioned into H_2O-mediated addition and inorganic-nucleophile-addition product classes according to their relative reaction rates. We also clarified the assumptions used for HMML/MAE uptake parameters, revised the MPAN + OH branching ratios following Nguyen et al. (2015), corrected and expanded the description of the aqueous-phase rate expressions, and updated all affected simulations, figures, tables, and attribution analyses. In addition, we expanded the discussion of remaining uncertainties, including core-shell morphology, phase separation, viscosity, product volatility, missing non-epoxide ISOA pathways, cloud-water chemistry, photolytic loss, and discrepancies in OSN-like product fractions.

Major Comments

Comment#1: I appreciate the authors for giving a comprehensive literature review on isoprene SOA chemistry and its impact. To further enhance its impact, it would be valuable to place this work within the context of previous

efforts to represent reactive uptake of epoxides in global models. Throughout the manuscript, several key studies (Jo et al., 2019, 2021; Liu et al., 2023; Zhang et al., 2025) are referenced, which form the foundation of the current framework and parameterizations. I suggest adding a dedicated paragraph that clearly summarizes what has been accomplished so far in global modeling, what this work contributes, and what gaps remain compared to regional models or measurements. This addition would be especially helpful for ACP's broad readership, many of whom may not be familiar with the current state of the literature on this topic. Such context would highlight the importance of this study and guide future research directions.

Response: We thank the reviewer for this constructive suggestion. We agree that placing this work more clearly within the context of previous global modeling efforts can improve the accessibility and broader relevance of the manuscript. In response, we have added a dedicated paragraph in the Introduction to summarize what has been accomplished so far in large-scale biogenic SOA modeling, what the present study contributes, and what gaps remain relative to regional models and measurements.

Specifically, we now describe that representations of biogenic SOA have evolved from simplified empirical or fixed-yield treatments used in early global models (Chung and Seinfeld, 2002; Chin et al., 2002), through semi-empirical two-product absorptive partitioning models (Odum et al., 1996; Griffin et al., 1999), to volatility-based gas–particle partitioning schemes (Donahue et al., 2006; Pye and Seinfeld, 2010), and more recently to explicit multiphase reactive uptake parameterizations for isoprene epoxides (Pye et al., 2013; Budisulistiorini et al., 2017; Jo et al., 2019, 2021; Ng et al., 2025). We also explain that these developments allow ISOA formation to respond more directly to aerosol liquid water, acidity, sulfate and other nucleophiles, and particle-phase reaction kinetics (Pye et al., 2013; Marais et al., 2016; Budisulistiorini et al., 2017; Jo et al., 2019, 2021).

We then clarify how the present study builds on these previous developments. The revised Introduction states that this work extends the CAM6-Chem framework by incorporating high-NOx epoxide precursors and subsequent heterogeneous reactions, distinguishing H_2O-mediated nucleophilic addition and inorganic-nucleophile-addition product classes, and evaluating how these updates affect ISOA composition and long-term ISOA trends over China. We further emphasize that this framework enables us to examine how ISOA trends are jointly controlled by precursor supply and heterogeneous reaction capacity across different regions. This motivation is particularly relevant for China, where emissions, meteorological conditions, and oxidation environments exhibit strong regional contrasts (Ding et al., 2016; Li et al., 2018; Wu et al., 2020; Yang et al., 2017).

Finally, we added discussion of the remaining limitations and gaps, including uncertainties in aerosol phase state, phase separation, organic-shell viscosity, diffusion limitations in the core-shell uptake treatment, limited kinetic constraints for HMML/MAE uptake, and assumptions related to ISOA yield and product volatility. These revisions have been incorporated in the Introduction (lines 95−120).

Lines 95−120:

Despite these advances, existing studies still rarely assess long-term ISOA changes by simultaneously considering pathway competition under different NOx emission backgrounds and the multiphase reaction environment. Given the large regional contrasts in emissions, meteorological conditions, and oxidation environments across China (Ding et al., 2016; Li et al., 2018; Wu et al., 2020; Yang et al., 2017), the dominant factors controlling ISOA formation and change are likely to differ by region. To further explore this question, a model framework is needed that can represent both low-NOx and high-NOx epoxide pathways and distinguish their major reaction branches and products. The continuous development of SOA representation in large-scale models provides an important foundation for this purpose. Representations of biogenic SOA have evolved from simplified empirical or fixed-yield treatments used in early global models (Chung and Seinfeld, 2002; Chin et al., 2002; Carlton et al., 2010; Kim et al., 2015), through semi-empirical two-product absorptive partitioning models (Odum et al., 1996; Griffin et al., 1999), to the Volatility Basis Set (VBS) approach (Donahue et al., 2006; Robinson et al., 2007; Pye and Seinfeld, 2010), and more recently to explicit multiphase reactive uptake parameterizations for isoprene epoxides (Pye et al., 2013; Budisulistiorini et al., 2017; Jo et al., 2019, 2021; Ng et al., 2025). These developments allow ISOA formation to respond more directly to aerosol liquid water, acidity, sulfate, and other nucleophiles, and particle-phase reaction kinetics (Pye et al., 2013; Marais et al., 2016; Budisulistiorini et al., 2017; Jo et al., 2019, 2021). Building on this progress, this study extends the CAM6-Chem framework by incorporating high-NOx epoxide precursors and subsequent heterogeneous reactions, distinguishing between H_2O-mediated nucleophilic addition and inorganic-nucleophile addition product classes, and evaluating how these updates affect ISOA composition and long-term ISOA trends over China. This framework further allows us to examine how ISOA trends are jointly controlled by precursor supply and heterogeneous reaction capacity across different regions. Nevertheless, important uncertainties remain in the current ISOA framework, including the simplified core-shell treatment of epoxide reactive uptake, uncertainties in aerosol phase state, organic-shell viscosity, phase separation, and diffusion limitations, as well as limited kinetic constraints for HMML/MAE uptake. Additional uncertainties arise from the assumptions of 100% ISOA yield and non-volatile epoxide-derived products, and from the possible omission of non-epoxide ISOA pathways in the current framework. Despite these remaining uncertainties, clarifying regional ISOA trends and controls can provide a scientific basis for evaluating how emission reductions jointly affect precursor supply and heterogeneous reaction environments, and for developing more targeted regional air-quality management strategies.

Budisulistiorini, S. H., Nenes, A., Carlton, A. G., Surratt, J. D., McNeill, V. F., and Pye, H. O. T.: Simulating aqueous-phase isoprene-epoxydiol (IEPOX) secondary organic aerosol production during the 2013 Southern Oxidant and Aerosol Study (SOAS), Environ. Sci. Technol., 51, 5026–5034, https://doi.org/10.1021/acs.est.6b05750, 2017.

Carlton, A. G., Bhave, P. V., Napelenok, S. L., Edney, E. O., Sarwar, G., Pinder, R. W., Pouliot, G. A., and Houyoux, M.: Model representation of secondary organic aerosol in CMAQv4.7, Environ. Sci. Technol., 44, 8553–8560, https://doi.org/10.1021/es100636q, 2010.

Chin, M., Ginoux, P., Kinne, S., Torres, O., Holben, B. N., Duncan, B. N., Martin, R. V., Logan, J. A., Higurashi, A., and Nakajima, T.: Tropospheric aerosol optical thickness from the GOCART model and comparisons with satellite and sun

photometer measurements, J. Atmos. Sci., 59, 461–483, https://doi.org/10.1175/1520-0469(2002)059<0461:TAOTFT>2.0.CO;2, 2002.
Chung, S. H. and Seinfeld, J. H.: Global distribution and climate forcing of carbonaceous aerosols, J. Geophys. Res.-Atmos., 107, 4407, https://doi.org/10.1029/2001JD001397, 2002.
Ding, X., He, Q.-F., Shen, R.-Q., Yu, Q.-Q., Zhang, Y.-Q., Xin, J.-Y., Wen, T.-X., and Wang, X.-M.: Spatial and seasonal variations of isoprene secondary organic aerosol in China: significant impact of biomass burning during winter, Sci. Rep., 6, 20411, https://doi.org/10.1038/srep20411, 2016.
Donahue, N. M., Robinson, A. L., Stanier, C. O., and Pandis, S. N.: Coupled partitioning, dilution, and chemical aging of semivolatile organics, Environ. Sci. Technol., 40, 2635–2643, https://doi.org/10.1021/es052297c, 2006.
Griffin, R. J., Cocker III, D. R., Flagan, R. C., and Seinfeld, J. H.: Organic aerosol formation from the oxidation of biogenic hydrocarbons, J. Geophys. Res.-Atmos., 104, 3555–3567, https://doi.org/10.1029/1998JD100049, 1999.
Jo, D. S., Hodzic, A., Emmons, L. K., Marais, E. A., Peng, Z., Nault, B. A., Hu, W., Campuzano-Jost, P., and Jimenez, J. L.: A simplified parameterization of isoprene-epoxydiol-derived secondary organic aerosol (IEPOX-SOA) for global chemistry and climate models: a case study with GEOS-Chem v11-02-rc, Geosci. Model Dev., 12, 2983–3000, https://doi.org/10.5194/gmd-12-2983-2019, 2019.
Jo, D. S., Hodzic, A., Emmons, L. K., Tilmes, S., Schwantes, R. H., Mills, M. J., Campuzano-Jost, P., Hu, W., Zaveri, R. A., Easter, R. C., Singh, B., Lu, Z., Schulz, C., Schneider, J., Shilling, J. E., Wisthaler, A., and Jimenez, J. L.: Future changes in isoprene-epoxydiol-derived secondary organic aerosol (IEPOX SOA) under the Shared Socioeconomic Pathways: the importance of physicochemical dependency, Atmos. Chem. Phys., 21, 3395–3425, https://doi.org/10.5194/acp-21-3395-2021, 2021.
Kim, P. S., Jacob, D. J., Fisher, J. A., Travis, K., Yu, K., Zhu, L., Yantosca, R. M., Sulprizio, M. P., Jimenez, J. L., Campuzano-Jost, P., Froyd, K. D., Liao, J., Hair, J. W., Fenn, M. A., Butler, C. F., Wagner, N. L., Gordon, T. D., Welti, A., Wennberg, P. O., Crounse, J. D., St. Clair, J. M., Teng, A. P., Millet, D. B., Schwarz, J. P., Markovic, M. Z., and Perring, A. E.: Sources, seasonality, and trends of southeast US aerosol: an integrated analysis of surface, aircraft, and satellite observations with the GEOS-Chem chemical transport model, Atmos. Chem. Phys., 15, 10411–10433, https://doi.org/10.5194/acp-15-10411-2015, 2015.
Li, J., Wang, G., Wu, C., Cao, C., Ren, Y., Wang, J., Li, J., Cao, J., Zeng, L., and Zhu, T.: Characterization of isoprene-derived secondary organic aerosols at a rural site in North China Plain with implications for anthropogenic pollution effects, Sci. Rep., 8, 535, https://doi.org/10.1038/s41598-017-18983-7, 2018.
Marais, E. A., Jacob, D. J., Jimenez, J. L., Campuzano-Jost, P., Day, D. A., Hu, W., Krechmer, J., Zhu, L., Kim, P. S., Miller, C. C., Fisher, J. A., Travis, K., Yu, K., Hanisco, T. F., Wolfe, G. M., Arkinson, H. L., Pye, H. O. T., Froyd, K. D., Liao, J., and McNeill, V. F.: Aqueous-phase mechanism for secondary organic aerosol formation from isoprene: application to the southeast United States and co-benefit of SO2 emission controls, Atmos. Chem. Phys., 16, 1603–1618, https://doi.org/10.5194/acp-16-1603-2016, 2016.
Ng, A. E., Chen, Y., Green, J., Farrell, S., Surratt, J. D., Ault, A. P., Turpin, B. J., and Vizuete, W. C.: Regional-scale modeling parameterizations for secondary organic aerosol formation from isoprene epoxydiols: experimentally based evaluation and optimization, ACS ES&T Air, 2, 2625–2637, https://doi.org/10.1021/acsestair.5c00258, 2025.
Odum, J. R., Hoffmann, T., Bowman, F., Collins, D., Flagan, R. C., and Seinfeld, J. H.: Gas/particle partitioning and secondary organic aerosol yields, Environ. Sci. Technol., 30, 2580–2585, https://doi.org/10.1021/es950943+, 1996.
Pye, H. O. T. and Seinfeld, J. H.: A global perspective on aerosol from low-volatility organic compounds, Atmos. Chem. Phys., 10, 4377–4401, https://doi.org/10.5194/acp-10-4377-2010, 2010.
Pye, H. O. T., Pinder, R. W., Piletic, I. R., Xie, Y., Capps, S. L., Lin, Y.-H., Surratt, J. D., Zhang, Z., Gold, A., Luecken, D. J., Hutzell, W. T., Jaoui, M., Offenberg, J. H., Kleindienst, T. E., Lewandowski, M., and Edney, E. O.: Epoxide pathways improve model predictions of isoprene markers and reveal key role of acidity in aerosol formation, Environ. Sci. Technol., 47, 11056–11064, https://doi.org/10.1021/es402106h, 2013.
Robinson, A. L., Donahue, N. M., Shrivastava, M. K., Weitkamp, E. A., Sage, A. M., Grieshop, A. P., Lane, T. E., Pierce, J. R., and Pandis, S. N.: Rethinking organic aerosols: semivolatile emissions and photochemical aging, Science, 315, 1259–1262, https://doi.org/10.1126/science.1133061, 2007.

Wu, K., Yang, X., Chen, D., Gu, S., Lu, Y., Jiang, Q., Wang, K., Ou, Y., Qian, Y., Shao, P., and Lu, S.: Estimation of biogenic VOC emissions and their corresponding impact on ozone and secondary organic aerosol formation in China, Atmos. Res., 231, 104656, https://doi.org/10.1016/j.atmosres.2019.104656, 2020.

Yang, Q., Yuan, Q., Li, T., Shen, H., and Zhang, L.: The relationships between PM2.5 and meteorological factors in China: seasonal and regional variations, Int. J. Environ. Res. Public Health, 14, 1510, https://doi.org/10.3390/ijerph14121510, 2017.

Comment#2: The authors make several assumptions in the epoxides' reactive uptake parameterizations particularly for HMML/MAE due to limited experimental constraints, which are understandable given limited experimental constraints. Some are explicitly stated such as diffusivity and solubility. Others are not clear and I'd appreciate further elaboration. For instance,

- 1. Are the same condensed-phase reaction constants for IEPOX applied to HMML/MAE? What is the literature basis for these choices?

Response: We thank the reviewer for raising this important point. Yes, in the current implementation, HMML and MAE are treated as IEPOX-like epoxide precursors, and the same solubility, diffusivity, and condensed-phase reaction constants used for IEPOX are applied to HMML and MAE. We agree that this assumption should be stated more explicitly and that its literature basis should be clarified. Following Jo et al. (2019, 2021), we adopted the IEPOX heterogeneous uptake framework. Because compound-specific multiphase kinetic constraints for HMML and MAE remain limited, our treatment follows previous modeling practice. Specifically, Pye et al. (2013) treated HMML like MAE in terms of heterogeneous uptake and assumed the particle-phase reaction rate constants of MAE to be the same as those of IEPOX due to the lack of kinetic data. Zhang et al. (2022) also noted that most HMML-related reaction parameters in models are commonly assumed to be the same as those for IEPOX. We therefore clarified in Sect. 2.1.2 that HMML and MAE are assigned the same solubility, diffusivity, and condensed-phase reaction constants as IEPOX in our implementation. We also added a statement to clarify the remaining uncertainty associated with this assumption. Although recent field-based studies have begun to constrain effective uptake-related parameters for IEPOX and lumped HMML/MAE, including pseudo-first-order heterogeneous reaction rate coefficients, reactive uptake coefficients, and aqueous-phase reaction parameter products (Zhu et al., 2025), a complete set of standalone compound-specific condensed-phase reaction constants for HMML and MAE remains unavailable. Therefore, this IEPOX-like treatment introduces uncertainty in the absolute uptake rates of HMML and MAE and may affect the modeled quantitative partitioning between high-NOx and low-NOx ISOA formation pathways. These revisions have been incorporated in Sect. 2.1.2 (lines 179−190), and the broader implications of this uncertainty are further discussed in Sect. 4 (lines 664−667).

Lines 179−190:

Due to limited laboratory constraints on the multiphase kinetics of HMML and MAE, HMML and MAE are treated as IEPOX-like epoxide precursors in the current implementation. This treatment is consistent with previous modeling practice. For example, Pye et al. (2013) treated HMML like MAE in terms of heterogeneous uptake and assumed the particle-phase reaction rate constants of MAE to be the same as those of IEPOX due to the lack of kinetic data. Zhang et al. (2022) also noted that most HMML-related reaction parameters in models are commonly assumed to be the same as those for IEPOX.

Following these studies, HMML and MAE are assigned the same solubility, diffusivity, and condensed-phase reaction constants as IEPOX in our implementation. Although a recent field-based study has estimated effective uptake parameters for IEPOX and lumped HMML/MAE, these constraints are not directly applicable here because they do not provide a complete set of standalone, compound-specific solubility, diffusivity, and branch-resolved condensed-phase reaction constants for HMML and MAE (Zhu et al., 2025). As a result, this IEPOX-like treatment introduces uncertainty in the absolute uptake rates of HMML and MAE and may affect the modeled quantitative partitioning between high-NOx and low-NOx ISOA formation pathways.

Lines 664−667:

HMML and MAE are also represented using the same solubility, diffusivity, and condensed-phase reaction parameters as IEPOX because compound-specific laboratory constraints remain limited. This IEPOX-like treatment introduces uncertainty in the absolute uptake rates of high-NOx epoxides and in the quantitative $ISOA_{HMML+MAE}/ISOA_{IEPOX}$ ratio.

- 2. How is the SOA speciation from epoxides calculated? Is it similar to Budisulistiorini et al. 2017 that uses the fraction of each nucleophilic addition rate to the total kaq?

Response: We thank the reviewer for this insightful comment. This question prompted us to carefully revisit the implementation of the formulation used to represent ISOA speciation from epoxide precursors in the original submission. In the initially submitted implementation, ISOA formation pathways for IEPOX, HMML, and MAE were represented as multiple parallel heterogeneous uptake reactions. Each product-forming pathway directly consumed the same gas-phase epoxide precursor using a distinct channel-specific reactive uptake coefficient derived from its respective aqueous-phase rate expression. As a result, ISOA speciation was effectively determined at the level of independent uptake fluxes, rather than being constrained by a single total uptake rate followed by internal partitioning among competing reaction channels. This approach allowed each channel to act as an independent sink of the precursor and resulted in the inorganic-nucleophile addition channel receiving an artificially enhanced share of gas-phase precursor uptake flux, leading to an overestimation of the corresponding inorganic-nucleophile addition products.

Following the reviewer's suggestion and consistent with Budisulistiorini et al. (2017), we have revised the formulation to a relative-rate branching framework. In essence, the implementation used in the original submission treated epoxide uptake as multiple parallel sinks, whereas the revised implementation treats it as a single total uptake process followed by competitive branching into different product classes.

In the revised implementation, a single total pseudo-first-order aqueous-phase rate constant $k_{aq,total}$ is first calculated as the sum of the particle-phase reaction channels (H_2O-mediated nucleophilic addition and inorganic-nucleophile addition channels) considered here: $k_{aq,total} = k_{H^+}[H^+] + k_{nuc}([SO_4^{2-}] + [NO_3^-])[H^+] + k_{HSO_4^-}[HSO_4^-]$. This total rate is used to compute the reactive uptake coefficient (γ) and the total uptake flux for each precursor. ISOA speciation is then determined

diagnostically by partitioning the total uptake flux according to the fractional contribution of each reaction channel to $k_{aq,total}$. Specifically, the branching ratio for the H_2O-mediated nucleophilic addition product class is calculated as $k_{aq,H_2O}/k_{aq,total} = k_{H^+}[H^+]/(k_{H^+}[H^+] + k_{nuc}([SO_4^{2-}] + [NO_3^-])[H^+] + k_{HSO_4^-}[HSO_4^-])$, whereas the branching ratio for the inorganic-nucleophile-addition product class is calculated as $k_{aq,SO_4/NO_3/HSO_4}/k_{aq,total} = (k_{nuc}([SO_4^{2-}] + [NO_3^-])[H^+] + k_{HSO_4^-}[HSO_4^-])/(k_{H^+}[H^+] + k_{nuc}([SO_4^{2-}] + [NO_3^-])[H^+] + k_{HSO_4^-}[HSO_4^-])$. The total particle-phase ISOA production is then distributed into H_2O-mediated nucleophilic addition products and inorganic-nucleophile addition products according to these branching ratios. This treatment ensures that the total uptake of each precursor is governed by the full particle-phase reaction rate constant, while the product distribution reflects the relative competition among nucleophilic addition pathways. This treatment is analogous to Budisulistiorini et al. (2017), who determined IEPOX-SOA speciation between tetrols and organosulfates based on the relative rates of precursor conversion to these products.

This revision leads to several noteworthy differences in the simulated results. First, the absolute concentrations of inorganic-nucleophile addition products (AIEOSN and AHMOSN) are reduced, as these species are no longer treated as independent uptake sinks but instead receive only their fractional share of the total epoxide uptake (Figure R3). Second, the relative contribution of individual ISOA subclasses is modified, reflecting a non-uniform redistribution between H_2O-mediated nucleophilic addition products and inorganic-nucleophile addition products (Figure R1). This leads to updated values in the trend attribution analysis and changes in the interannual variability of specific ISOA components (Figure R2 and Figure R4), as these diagnostics depend on how ISOA is partitioned among chemically distinct formation pathways, rather than on a simple uniform scaling of total ISOA. Third, the regression-based attribution coefficients for the driving factors considered are revised, leading to updated quantitative estimates in the trend decomposition. The revised regression coefficients are reported in Table 1 of the revised manuscript and Table S1 in the revised Supplement. The figures shown below are selected representative examples illustrating the major changes in absolute concentrations, relative contributions, interannual variability, and long-term trends. All other affected results, figures, tables, and quantitative analyses have also been updated accordingly in the revised manuscript and supplement.

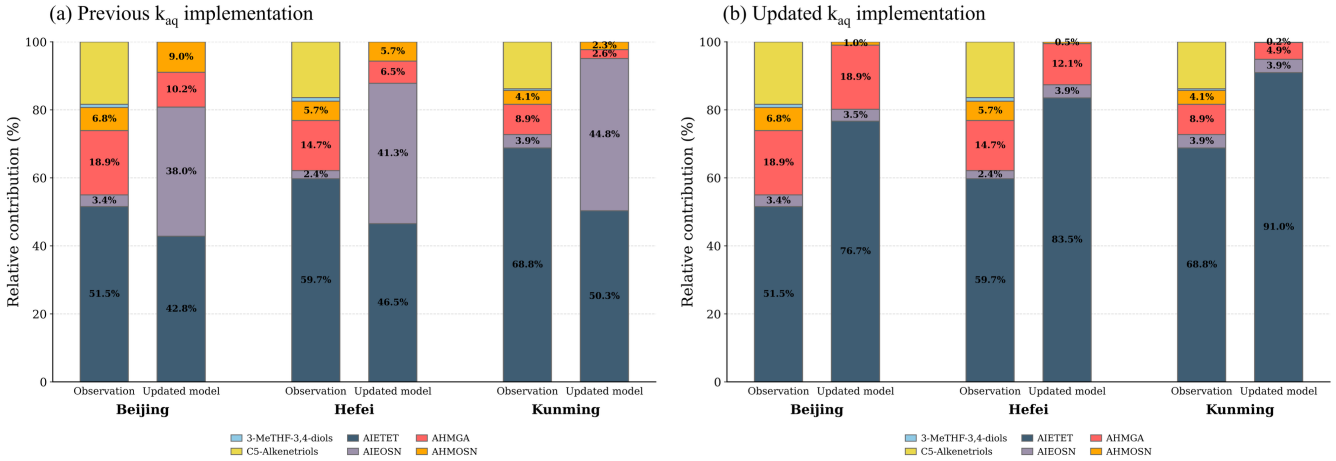

Figure R1: Comparison of ISOA product composition between ground-based observations adapted from Zhang et al. (2022) and the model simulation in this study, corresponding to the observation-model comparison shown in the original Figure 2c in the manuscript. The grouped stacked bars show the relative contribution of each ISOA product to total measured or simulated ISOA at Beijing, Hefei, and Kunming. For each city, the left bar represents the observed composition and the right bar represents the corresponding model simulation. Panel (a) shows results obtained with the previous k_{aq} implementation, in which product-forming pathways were treated as independent uptake sinks. Panel (b) shows results obtained with the updated k_{aq} implementation, in which total epoxide uptake is first calculated and then partitioned among product classes using the relative-rate branching framework.

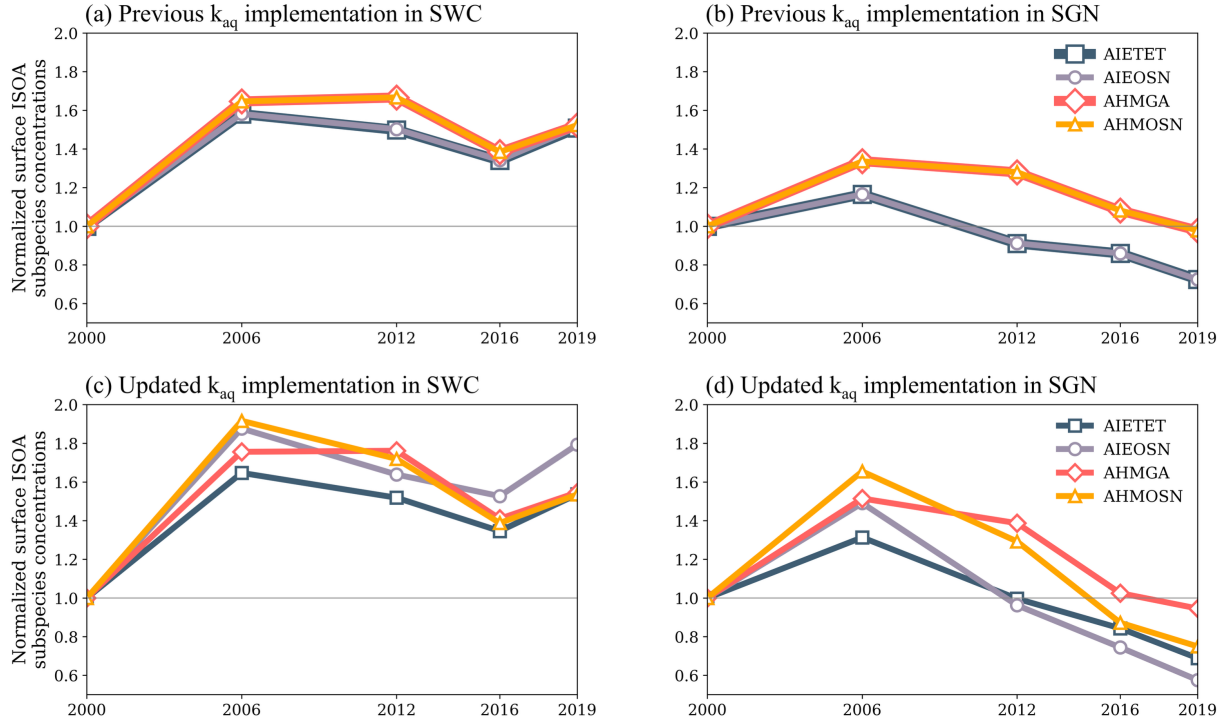

Figure R2: Comparison of the time series of normalized surface isoprene-derived secondary organic aerosol (ISOA) subspecies concentrations corresponding to the original Figure 8a in the manuscript. Results are shown for Southwest China (SWC) and the

Shaanxi−Gansu−Ningxia region (SGN). Panels (a) and (b) show results obtained with the previous k_{aq} implementation, in which product-forming pathways were treated as independent uptake sinks, for SWC and SGN, respectively, whereas panels (c) and (d) show the corresponding results obtained with the updated k_{aq} implementation, in which total epoxide uptake is first calculated and then partitioned among product classes using the relative-rate branching framework. The normalized values are calculated as the ratio of the value in each year to that in 2000. AIETET, AIEOSN, AHMGA, and AHMOSN are shown in dark blue, gray-purple, rose red, and orange, respectively.

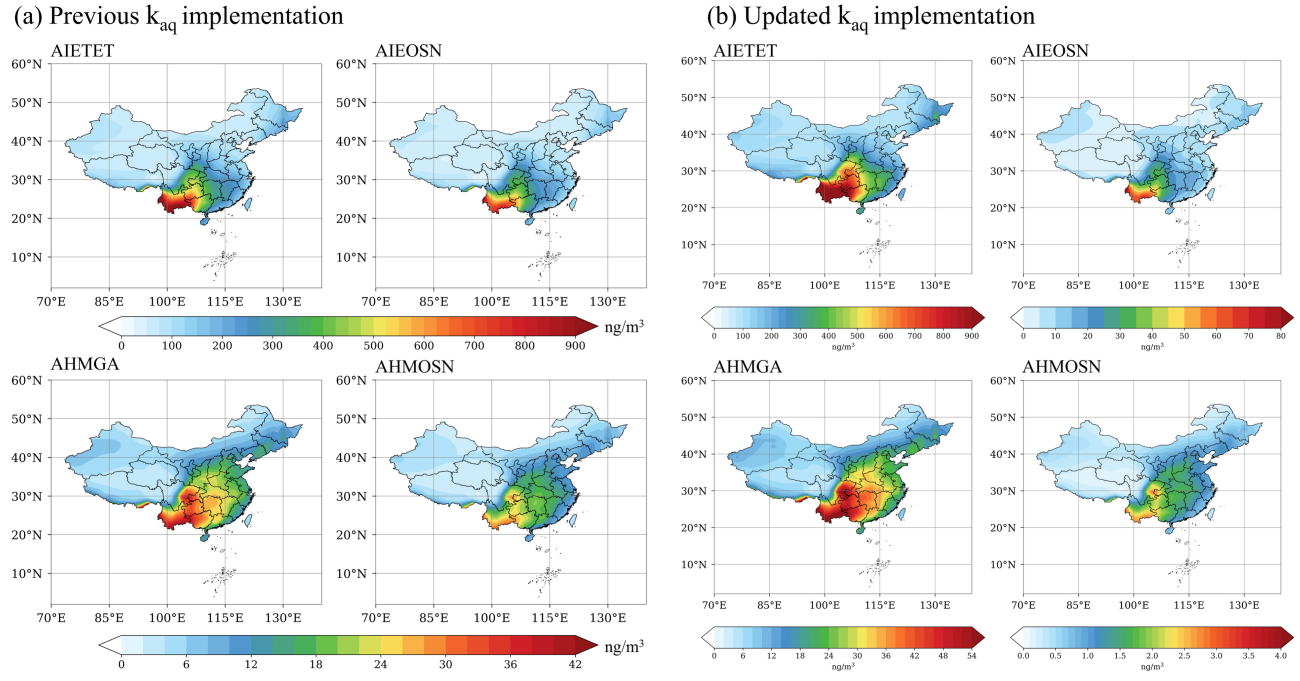

Figure R3: Comparison of annual mean surface concentrations of four isoprene-derived secondary organic aerosol (ISOA) subspecies (AIETET, AIEOSN, AHMGA, and AHMOSN) over China, averaged over the five simulation years (2000, 2006, 2012, 2016, and 2019) (unit: ng m^{-3}), corresponding to the original Figure S1 in the Supplement. Panel (a) shows results obtained with the previous k_{aq} implementation, in which product-forming pathways were treated as independent uptake sinks, while panel (b) shows results obtained with the updated k_{aq} implementation, in which total epoxide uptake is first calculated and then partitioned among product classes using the relative-rate branching framework.

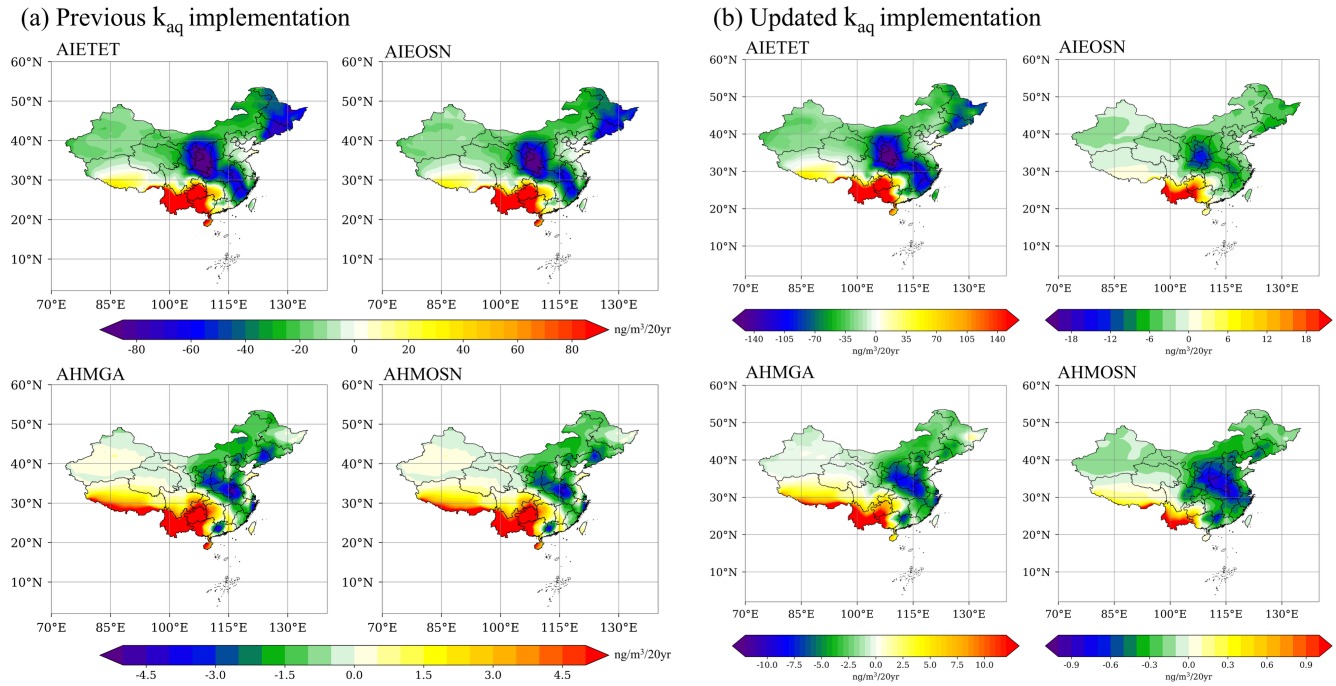

Figure R4: Comparison of long-term trends in annual mean surface concentrations of four isoprene-derived secondary organic aerosol (ISOA) subspecies (AIETET, AIEOSN, AHMGA, and AHMOSN) surface concentrations (ng m^{-3} per 20 years) in China from 2000 to 2019, corresponding to the original Figure S4 in the Supplement. Panel (a) shows results obtained with the previous k_{aq} implementation, in which product-forming pathways were treated as independent uptake sinks, while panel (b) shows results obtained with the updated k_{aq} implementation, in which total epoxide uptake is first calculated and then partitioned among product classes using the relative-rate branching framework.

Importantly, these updates do not alter the core conclusions of the study. The revised implementation primarily affects the quantitative partitioning among ISOA subspecies and the corresponding numerical values in the attribution analysis, while the main scientific interpretations remain unchanged: the updated mechanism improves the representation of ISOA magnitude and composition in CAM6-Chem; IEPOX remains the dominant ISOA formation pathway at the national scale, although the HMML/MAE pathway becomes more important regionally and seasonally under high-NOx conditions; and the long-term ISOA trend over China remains slightly negative at the national scale but shows strong regional heterogeneity, with increases in SWC mainly associated with enhanced biogenic isoprene emissions and decreases in SGN mainly associated with declining sulfate. We have revised the relevant discussion and conclusions throughout the manuscript and supplement accordingly. The revised description of the updated model implementation is provided in Sect. 2.12, lines 196–242.

Lines 196–242:

Subsequently, following the resistor model equation of Gaston et al. (2014), this study calculates the reactive uptake coefficient γ for IEPOX, HMML, and MAE (Gaston et al., 2014). The governing expression is:

$$\frac{1}{\gamma} = \frac{\omega R_p}{4D_{gas}} + \frac{1}{\alpha} + \frac{\omega R_p}{4RTH_{org}D_{org}(q_{org}F-1)}, \quad (1)$$

Where γ represents the reactive uptake coefficient, ω is the mean molecular speed of epoxides (m s^{-1}), R_p is the particle radius (m), D_{gas} is the gas-phase diffusion coefficient of epoxides (10^{-5} m^2 s^{-1}), α is the mass accommodation coefficient (0.1), R is the universal gas constant (8.2057 x 10^{-2} L atm mol^{-1} K^{-1}), T is temperature (K), H_{org} is the Henry's law coefficient in the organic layer (2 x 10^6 M atm^{-1}), and D_{org} is the diffusion coefficient of epoxides in the organic layer. The term F is calculated as:

$$F = \frac{\coth(q_{org}) + h(q_{aq}, q^*_{org})}{1 + \coth(q_{org})h(q_{aq}, q^*_{org})}, \quad (2)$$

Where the function $h(q_{aq}, q^*_{org})$ is given by:

$$h(q_{aq}, q^*_{org}) = -\tanh(q^*_{org}) \frac{\frac{H_{aq}D_{aq}}{H_{org}D_{org}}(q_{aq}\coth(q_{aq}) - 1) - (q^*_{org}\coth(q^*_{org}) - 1)}{\frac{H_{aq}D_{aq}}{H_{org}D_{org}}(q_{aq}\coth(q_{aq}) - 1) - (q^*_{org}\tanh(q^*_{org}) - 1)}, \quad (3)$$

Here, H_{aq} is the Henry's law coefficient in the aqueous core (1.7 x 10^7 M atm^{-1}), and D_{aq} is the diffusion coefficient of epoxides in the aqueous core (10^{-9} m^2 s^{-1}). The variables q_{org}, q_{aq}, and q^*_{org} are defined as:

$$q_{org} = R_p\sqrt{\frac{k_{org}}{D_{org}}}, \quad (4)$$

$$q_{aq} = R_c\sqrt{\frac{k_{aq,total}}{D_{aq}}}, \quad (5)$$

$$q^*_{org} = \frac{R_C}{R_p} q_{org}, \quad (6)$$

Where R_C is the inorganic aqueous core radius (m), k_{org} is the pseudo-first-order reaction rate constant of epoxides in the organic shell (s^{-1}), and $k_{aq,total}$ is the total pseudo-first-order aqueous-phase reaction rate constant (s^{-1}), calculated as the sum of all particle-phase reaction channels that consume each precursor:

$$k_{aq,total} = k_{H^+}[H^+] + k_{nuc}([SO_4^{2-}] + [NO_3^-])[H^+] + k_{HSO_4^-}[HSO_4^-], \quad (7)$$

The first term represents the acid-catalyzed ring-opening followed by nucleophilic addition of aerosol liquid water, leading to H_2O-mediated nucleophilic addition products. Here, k_{H^+} is the corresponding effective H_2O-mediated nucleophilic addition rate constant (0.036 M^{-1} s^{-1}), with aerosol liquid water treated as the solvent and included implicitly, and $[H^+]$ is the proton concentration (M). The second term represents acid-catalyzed ring opening followed by nucleophilic addition of sulfate and nitrate ions, leading to organosulfates and organonitrates. Here, k_{nuc} is the third-order rate constant for sulfate- and nitrate-addition reactions (2 x 10^{-4} M^{-2} s^{-1}), and $([SO_4^{2-}] + [NO_3^-])$ is the concentration of sulfate and nitrate ions (M).

The third term represents concerted protonation and nucleophilic addition by bisulfate, leading to organosulfates. $k_{HSO_4^-}$ is the reaction rate constant due to the presence of bisulfate (7.3×10^{-4} M^{-1} s^{-1}), and $[HSO_4^-]$ is the bisulfate concentration (M).

For each precursor considered here, including IEPOX, HMML, and MAE, $k_{aq,total}$ is used to calculate the reactive uptake coefficient and the total uptake flux. The resulting particle-phase ISOA production is then distributed into the H_2O-mediated nucleophilic addition and inorganic-nucleophile addition product classes according to the relative contribution of each reaction channel to $k_{aq,total}$. The H_2O-mediated nucleophilic addition class is represented by the $k_{H^+}[H^+]$ channel, whereas the inorganic-nucleophile addition class combines the sulfate-, nitrate-, and bisulfate-assisted channels, which are collectively represented by $k_{nuc}([SO_4^{2-}] + [NO_3^-])[H^+] + k_{HSO_4^-}[HSO_4^-]$. The corresponding branching ratios for the two product classes are defined as BR_{H_2O} and $BR_{SO_4/NO_3/HSO_4}$, respectively:

$$BR_{H_2O} = \frac{k_{aq,H_2O}}{k_{aq,total}} = \frac{k_{H^+}[H^+]}{k_{aq,total}} \quad (8)$$

$$BR_{SO_4/NO_3/HSO_4} = \frac{k_{aq,SO_4/NO_3/HSO_4}}{k_{aq,total}} = \frac{k_{nuc}([SO_4^{2-}]+[NO_3^-])[H^+]+k_{HSO_4^-}[HSO_4^-]}{k_{aq,total}} \quad (9)$$

This relative-rate branching treatment follows the approach of Budisulistiorini et al. (2017), in which $ISOA_{IEPOX}$ speciation between tetrols and organosulfates was determined from the relative rates of precursor conversion to these products. This study follows the approach of Jo et al. (2021), where the reactivity of epoxides in the organic shell was parameterized with the same reaction rate constant as in the aqueous phase (k_{org}=$k_{aq,total}$). This treatment follows the Jo et al. (2019, 2021) core-shell framework and represents a simplifying assumption, because phase separation, organic-shell viscosity, and differences in acidity between the inorganic core and organic shell may alter epoxide diffusion and reactivity (Schmedding et al., 2020; Farrell et al., 2025). Furthermore, considering the strong sensitivity of D_{org} to relative humidity (RH) in the atmosphere, this study accounts for the RH dependence of D_{org}, as described in Table S3 of Zhang et al. (2018) (Zhang et al., 2018).

- 3. The parameterization appears to assume a core-shell morphology with organic shell and inorganic core. It may be problematic to assume epoxides have same reactivity in both phases, as previous work (Zhang et al., 2019; Chen et al., 2024) indicate.

Zhang, Yue, Yuzhi Chen, Ziying Lei, et al. "Joint Impacts of Acidity and Viscosity on the Formation of Secondary Organic Aerosol from Isoprene Epoxydiols (IEPOX) in Phase Separated Particles." ACS Earth and Space Chemistry 3, no. 12 (2019): 2646-58. https://doi.org/10.1021/acsearthspacechem.9b00209.

Chen, Yuzhi, Alexandra E. Ng, Jaime Green, et al. "Applying a Phase-Separation Parameterization in Modeling Secondary Organic Aerosol Formation from Acid-Driven Reactive Uptake of Isoprene Epoxydiols under Humid Conditions." ACS ES&T Air 1, no. 6 (2024): 511–24. https://doi.org/10.1021/acsestair.4c00002.

Response: We thank the reviewer for this important comment. We agree that the core-shell treatment and the assumption of identical reactivity in the organic shell and aqueous core represent important simplifications in the current reactive uptake

parameterization. In the revised manuscript, we have clarified in Sect. 2.1.2 that the model follows the Jo et al. (2019, 2021) core-shell framework, in which the reactivity of epoxides in the organic shell is parameterized using the same effective reaction rate coefficient as in the aqueous phase. We now explicitly state that this treatment should be regarded as a simplifying assumption because phase separation, organic-shell viscosity, and differences in acidity between the inorganic core and organic shell may alter epoxide diffusion and reactivity. We have also expanded the discussion in Sect. 3.1 and the limitation discussion in Sect. 4 to address the implications of this assumption. Specifically, we now discuss that phase separation and viscous organic coatings may impose additional diffusion limitations on epoxide reactive uptake; therefore, the assumption of identical reactivity in both phases may lead to overestimation of epoxide-derived ISOA under conditions with strong phase separation or highly viscous organic coatings. These revisions have been incorporated in Sect. 2.1.2 (lines 235–240), Sect. 3.1 (lines 308−312), and Sect. 4 (lines 660−664). We also thank the reviewer for pointing us to the relevant studies by Zhang et al. (2019) and Chen et al. (2024b), which have been incorporated into the revised manuscript to support the discussion.

Lines 235−240:

This study follows the approach of Jo et al. (2021), where the reactivity of epoxides in the organic shell was parameterized with the same reaction rate constant as in the aqueous phase (k_{org}=$k_{aq,total}$). This treatment follows the Jo et al. (2019, 2021) core-shell framework and represents a simplifying assumption, because phase separation, organic-shell viscosity, and differences in acidity between the inorganic core and organic shell may alter epoxide diffusion and reactivity (Schmedding et al., 2020; Farrell et al., 2025).

Lines 308−312:

In particular, the current core-shell uptake treatment assumes the same reaction rate coefficient in the organic shell and aqueous core. If phase separation and viscous organic coatings impose stronger diffusion limitations than represented here, effective epoxide uptake may be reduced in the real atmosphere, and the model may overestimate ISOA formation, especially under conditions with high organic coatings or strong phase separation.

Lines 660−664:

As described in Sect. 2.1.2, the model follows a core-shell treatment in which the organic shell and aqueous core are assumed to have the same reaction rate coefficient. Because phase separation and increased organic-shell viscosity can limit epoxide diffusion and reactive uptake, this assumption may overestimate epoxide-derived ISOA under strongly phase-separated or highly viscous conditions (Zhang et al., 2019; Schmedding et al., 2020; Chen et al., 2024b; Farrell et al., 2025).

Chen, Y., Ng, A. E., Green, J., Zhang, Y., Riva, M., Riedel, T. P., Pye, H. O. T., Lei, Z., Olson, N. E., Cooke, M. E., Zhang, Z., Vizuete, W., Gold, A., Turpin, B. J., Ault, A. P., and Surratt, J. D.: Applying a phase-separation parameterization in modeling secondary organic aerosol formation from acid-driven reactive uptake of isoprene epoxydiols under humid conditions, ACS ES&T Air, 1, 511–524, https://doi.org/10.1021/acsestair.4c00002, 2024.

Jo, D. S., Hodzic, A., Emmons, L. K., Marais, E. A., Peng, Z., Nault, B. A., Hu, W., Campuzano-Jost, P., and Jimenez, J. L.: A simplified parameterization of isoprene-epoxydiol-derived secondary organic aerosol (IEPOX-SOA) for global chemistry and climate models: a case study with GEOS-Chem v11-02-rc, Geosci. Model Dev., 12, 2983–3000, https://doi.org/10.5194/gmd-12-2983-2019, 2019.

Jo, D. S., Hodzic, A., Emmons, L. K., Tilmes, S., Schwantes, R. H., Mills, M. J., Campuzano-Jost, P., Hu, W., Zaveri, R. A., Easter, R. C., Singh, B., Lu, Z., Schulz, C., Schneider, J., Shilling, J. E., Wisthaler, A., and Jimenez, J. L.: Future changes in isoprene-epoxydiol-derived secondary organic aerosol (IEPOX SOA) under the Shared Socioeconomic Pathways: the importance of physicochemical dependency, Atmos. Chem. Phys., 21, 3395–3425, https://doi.org/10.5194/acp-21-3395-2021, 2021.

Zhang, Y., Chen, Y., Lei, Z., Olson, N. E., Riva, M., Koss, A. R., Zhang, Z., Gold, A., Jayne, J. T., Worsnop, D. R., Onasch, T. B., Kroll, J. H., Turpin, B. J., Ault, A. P., and Surratt, J. D.: Joint impacts of acidity and viscosity on the formation of secondary organic aerosol from isoprene epoxydiols (IEPOX) in phase-separated particles, ACS Earth Space Chem., 3, 2646–2658, https://doi.org/10.1021/acsearthspacechem.9b00209, 2019.

Please clarify these assumptions and critically discuss potential uncertainties they introduce when evaluating against observations and long-term trend analyses later in the manuscript. It would also be helpful to add discussion on these uncertainties as limitations towards the end of the manuscript.

Response: We thank the reviewer for these detailed and constructive questions. In addition to the clarifications above, we have added a limitations discussion in Sect. 4 to clarify how these assumptions may affect the evaluation against observations and the interpretation of long-term trend analyses. We now state that the IEPOX-like treatment of HMML/MAE, the core-shell assumption of identical reactivity in the organic and aqueous phases, and the assumptions of 100 % SOA yield and non-volatile products may influence the absolute ISOA magnitude, pathway partitioning, sensitivity to sulfate/aerosol liquid water/acidity, and quantitative trend attribution. Accordingly, pathway-specific contributions and regression-based trend attributions are interpreted as diagnostic results under the adopted chemical framework rather than exact causal contributions independent of these model assumptions. These additions have been incorporated in Sect. 4 (lines 659−677).

Lines 659−677:

Future model development should further address several simplifying assumptions in the current epoxide reactive uptake parameterization. As described in Sect. 2.1.2, the model follows a core-shell treatment in which the organic shell and aqueous core are assumed to have the same reaction rate coefficient. Because phase separation and increased organic-shell viscosity can limit epoxide diffusion and reactive uptake, this assumption may overestimate epoxide-derived ISOA under strongly phase-separated or highly viscous conditions (Zhang et al., 2019; Schmedding et al., 2020; Chen et al., 2024b; Farrell et al., 2025). HMML and MAE are also represented using the same solubility, diffusivity, and condensed-phase reaction parameters as IEPOX because compound-specific laboratory constraints remain limited. This IEPOX-like treatment introduces uncertainty in the absolute uptake rates of high-NOx epoxides and in the quantitative $ISOA_{HMML+MAE}/ISOA_{IEPOX}$ ratio. The assumptions of 100% ISOA yield from epoxide reactive uptake and non-volatile epoxide-derived ISOA introduce additional uncertainty, although they are consistent with previous global ISOA modeling studies (Marais et al., 2016; Jo et al., 2019, 2021). Lower effective yields or partial volatility, especially for products such as 2-MT and 2-MGA, could reduce

simulated ISOA concentrations and their sensitivity to sulfate, aerosol liquid water, and acidity. Consistent with this need, gas–particle partitioning treatments for 2-MT in regional models suggest a useful direction for future improvement in global models (Pye et al., 2018; Shrivastava et al., 2022). Finally, the removal of ISOA formation from the VBS scheme may also remove important non-epoxide contributions to ISOA that were previously represented implicitly, such as multifunctional organic peroxides under low-NOx conditions and organic nitrates under high-NOx conditions (Paulot et al., 2009a; Schwantes et al., 2019). Taken together, these assumptions mean that the long-term trends and regression-based attributions diagnosed here should be interpreted within the adopted epoxide-focused chemical framework, rather than as exact causal contributions independent of model structure and parameterization

Comment#3: The evaluation against measurements shows improved mass closure relative to the author's previous work. However, the authors did not address the non-negligible discrepancies observed in the OSN subspecies. While the model predicted a more even distribution of water and sulfate added products, measurements show that OSN contributes very little. Other measurements such as He et al. (2018) reported similar findings. While uncertainties in measurements exist, this could also suggest uncertainties in the reactive uptake parameterization, possible missing processes, or inaccurate representation of the heterogeneous reaction medium (such as varying abundances of different nucleophiles). These points are related to previous comments about the assumptions used in the current parameterization. It would be helpful to discuss potential reasons for this gap and how future parameterization or additional measurements might address the gap.

He, Quan-Fu, Xiang Ding, Xiao-Xin Fu, et al. "Secondary Organic Aerosol Formation From Isoprene Epoxides in the Pearl River Delta, South China: IEPOX- and HMML- Derived Tracers." Journal of Geophysical Research: Atmospheres 123, no. 13 (2018): 6999–7012. https://doi.org/10.1029/2017JD028242.

Response: We thank the reviewer for this insightful comment. We agree that the OSN-like subspecies simulated in the initially submitted implementation required further clarification. As discussed above in our response to the second part of Comment#2, the apparent overestimation of OSN-like products was likely related to the parallel-sink treatment used in the initially submitted implementation of the updated epoxide-derived ISOA mechanism. In that initially submitted implementation, H_2O-mediated nucleophilic addition and inorganic-nucleophile addition were represented as separate product-forming pathways that independently consumed the same gas-phase epoxide precursor. This treatment could produce a more even distribution between water-addition products and OSN-like products than suggested by molecular tracer observations.

To address this issue, we revisited the treatment of epoxide-derived product formation and replaced the initially submitted parallel-sink treatment with a relative-rate branching framework following Budisulistiorini et al. (2017). The detailed formulation and branching-ratio calculation are provided in our response to the second part of Comment#2 and have been incorporated into the revised model description in Sect. 2.1.2. In the revised implementation, the total pseudo-first-order aqueous-phase reaction rate constant is calculated as the sum of all particle-phase reaction channels that consume each epoxide precursor, and the resulting epoxide-derived ISOA production is then allocated to H_2O-mediated nucleophilic addition and inorganic-nucleophile addition products according to their fractional contributions to the total reaction rate.

This update substantially changes the simulated product distribution. As shown in Figure R1, the initially submitted implementation produced a relatively large contribution from OSN-like products, particularly AIEOSN and AHMOSN, whereas the revised relative-rate branching treatment greatly reduces their simulated contributions. In the revised implementation, AIETET becomes the dominant simulated ISOA product at Beijing, Hefei, and Kunming, and the combined contribution of AIEOSN and AHMOSN is reduced to only a few percent. This revised product distribution is more consistent with the molecular tracer observations used for model evaluation and with previous field measurements showing relatively small OSN contributions, such as He et al. (2018).

We have revised the corresponding model-observation comparison in the manuscript and present the comparison between the initially submitted and revised results in Figure R1 of this response. We also added discussion in Sect. 3.1 and Sect. 4 to clarify the remaining uncertainties associated with the representation of epoxide-derived product formation. Although the revised branching treatment substantially reduces the OSN-like contribution simulated in the initially submitted implementation, remaining discrepancies between simulated and observed individual product fractions may still reflect uncertainties in pathway branching, reactive uptake parameters, mass transfer, aerosol phase state, and possible missing competing formation or loss processes. In particular, assumptions related to the core-shell uptake treatment, organic-shell viscosity, phase separation, product volatility, and the limited compound-specific constraints for HMML/MAE may affect the simulated abundance and partitioning of individual ISOA products. Future improvements will require better observational and laboratory constraints on epoxide-specific uptake parameters, aerosol phase state and diffusion limitations, product yields and volatility, as well as improved representation of potential non-epoxide ISOA formation pathways under atmospherically relevant aerosol conditions. These revisions have been incorporated in Sect. 3.1 (lines 299−314) and Sect. 4 (lines 659−677).

Lines 299−314:

Several factors may contribute to these positive biases. First, missing or simplified competing loss pathways may cause an over-allocation of epoxide precursors to the explicitly represented ISOA products. For example, a fraction of IEPOX-derived products in the real atmosphere may be diverted to C5-alkene triols or other particle-phase products that are not explicitly represented here, thereby reducing the effective yield of AIETET (Pye et al., 2013). In addition, previous studies have shown that AIETET and AHMGA are sensitive to factors such as pathway branching, mass transfer, reaction kinetics, and aerosol phase state. For example, uncertainties in the relative rates of water addition versus organosulfate formation can affect the predicted product distribution between 2-MT and organosulfate products (Budisulistiorini et al., 2017). Similarly, assumptions related to aerosol phase state, organic-shell viscosity, and phase separation can influence IEPOX reactive uptake and may affect the simulated abundance of IEPOX-derived tracers (Zhang et al., 2018, 2019; Chen et al., 2024b). In particular, the current core-shell uptake treatment assumes the same reaction rate coefficient in the organic shell and aqueous

core. If phase separation and viscous organic coatings impose stronger diffusion limitations than represented here, effective epoxide uptake may be reduced in the real atmosphere, and the model may overestimate ISOA formation, especially under conditions with high organic coatings or strong phase separation. For AHMGA, uncertainties in the multiphase uptake and reaction parameters of HMML/MAE may also contribute to the model bias, because compound-specific constraints for these high-NOx epoxides remain limited (Zhang et al., 2022; Zhu et al., 2025).

Others Comments

Comment#4: Lines 110-112: What is the chemical nature of the IVOCs and SVOCs mentioned here apart from the already mentioned anthropogenic and biogenic emissions? Do they involve in gas- and aerosol-phase reactions in the model?

Response: We thank the reviewer for this helpful question. We have clarified the chemical nature and model treatment of IVOCs and SVOCs in Sect. 2.1.1. In this study, IVOCs and SVOCs are not treated as explicitly speciated molecular compounds, but as lumped lower-volatility organic precursor classes defined by volatility. Their emissions are scaled from POA and NMVOC emissions following the default CAM6-Chem treatment described by Chang et al. (2022), Tilmes et al. (2019), and Zhang et al. (2025). We also clarified that IVOCs and SVOCs are included in the default CAM6-Chem VBS SOA scheme, which was not modified in this study. In this scheme, organic precursors including IVOCs and SVOCs are oxidized to volatile SOA gaseous precursors, which subsequently partition between the gas and aerosol phases. Therefore, IVOCs and SVOCs are involved in the default VBS-based gas-phase oxidation and gas-particle partitioning treatment, but they are not part of the newly added explicit epoxide reactive uptake chemistry. These clarifications have been incorporated in Sect. 2.1.1 (lines 128−133 and lines 140−144).

Line 128−133:

In this study, intermediate-volatility organic compounds (IVOCs) and semi-volatile organic compounds (SVOCs) represent lumped lower-volatility organic precursor classes defined by volatility rather than explicitly speciated molecular structures. Emissions of IVOCs and SVOCs are scaled from primary organic aerosol (POA) and non-methane volatile organic compounds (NMVOCs) emissions (Chang et al., 2022; Tilmes et al., 2019). The specific scaling equations and coefficients are described in the supplement of Zhang et al. (2025) (Eqs. A1–A3).

Lines 140−144:

Organic compounds (including glyoxal, monoterpenes, sesquiterpenes, benzene, toluene, lumped xylenes, IVOCs, and SVOCs) are oxidized to form gas-phase SOA precursors in five volatility bins, with effective saturation concentrations (C*, at 300 K) of 0.01, 0.1, 1.0, 10.0, and 100.0 μg m^{-3}. These precursors subsequently partition between the gas and particle phases (Tilmes et al., 2019). This VBS treatment follows the default CAM6-Chem SOA scheme and was not modified in this study.

Comment#5: Lines 125-126: I understand it is impossible to include every new mechanism altogether in the models. It is worth noting that isoprene SOA photolysis is faster than MT-SOA. The model-ready rate is reported in Zawadowicz et al. (2020) and shown to have a huge impact on reducing isoprene SOA over Amazon.

Zawadowicz, Maria A., Ben H. Lee, Manish Shrivastava, et al. "Photolysis Controls Atmospheric Budgets of Biogenic Secondary Organic Aerosol." Environmental Science & Technology 54, no. 7 (2020): 3861–70. https://doi.org/10.1021/acs.est.9b07051.

Response: We thank the reviewer for pointing out this important process. We agree that photolytic loss of isoprene-derived SOA may introduce additional uncertainty in the simulated ISOA lifetime and burden. In the revised manuscript, we have added a discussion in Sect. 4 noting that Zawadowicz et al. (2020) reported faster photolysis of isoprene SOA than monoterpene-derived SOA, suggesting that this process may affect the simulated ISOA lifetime and abundance. We have also clarified that further refinement of the SOA chemical mechanism, including improved representation of such processes, is needed to reduce the remaining uncertainties and biases in key ISOA subspecies. This revision has been incorporated in Sect. 4 (lines 680−684).

Lines 680−684:

These include isoprene cloud-water chemistry, which may provide an additional ISOA source and influence simulated aerosol composition, and photolytic loss, since ISOA may photolyze faster than monoterpene-derived SOA (Zawadowicz et al., 2020), thereby affecting its simulated lifetime and burden. Incorporating these missing formation and loss processes, together with more composition-resolved observations to constrain pathway-specific chemistry, will be important for future model refinement.

Comment#6: Line 143-144: The branching ratios 0.57 vs 0.21 are not consistent with previous experimental work by Nguyen et al., MPAN + OH predominantly produces HMML (~75%) and the MAE yield is minor (< 2%). Please clarify. Line 143-144: The branching ratios (0.57 vs 0.21) differ from Nguyen et al.'s findings, where MPAN + OH mainly produces HMML (~75%) with a minor MAE yield (< 2%). Please explain.

Nguyen, Tran B., Kelvin H. Bates, John D. Crounse, et al. "Mechanism of the Hydroxyl Radical Oxidation of Methacryloyl Peroxynitrate (MPAN) and Its Pathway toward Secondary Organic Aerosol Formation in the Atmosphere." Physical Chemistry Chemical Physics: PCCP 17, no. 27 (2015): 17914–26. https://doi.org/10.1039/c5cp02001h.

Response: We thank the reviewer for pointing this out. In the original implementation, the molar branching ratios for HMML and MAE formation from the MPAN + OH pathway were set to 0.57 and 0.21, respectively, following the CRACMM1 gas-phase chemical mechanism used in CMAQ. However, after revisiting the experimental constraints highlighted by the reviewer, we agree that the product distribution reported by Nguyen et al. (2015) provides a more direct constraint for the MPAN + OH pathway considered here. Therefore, following Nguyen et al. (2015), we have revised the branching ratios to 0.75 for HMML and 0.02 for MAE. We have updated the model implementation accordingly and regenerated all related simulation results, figures, and quantitative analyses using the revised branching ratios. The change leads to only very small

differences in the simulated HMML + MAE concentrations and spatial distribution (Figure R5), and does not materially affect the overall conclusions, because the main analyses in this study focus on the combined HMML + MAE concentrations rather than the two individual precursors. As shown in Figure R5, the mean annual surface concentrations of combined HMML and MAE in China from 2000 to 2019 are nearly unchanged between the initially submitted branching ratios (HMML/MAE = 0.57/0.21) and the revised branching ratios constrained by Nguyen et al. (2015) (HMML/MAE = 0.75/0.02). However, it provides a more experimentally constrained representation of the relative importance of the HMML and MAE branches. The corresponding description in Sect. 2.1.2 has been revised (lines 168−170), and the updated chemical reactions and branching ratios, based on the experimental results reported by Nguyen et al. (2015), are now listed in Table S2. All affected results throughout the manuscript and Supplement have been updated accordingly.

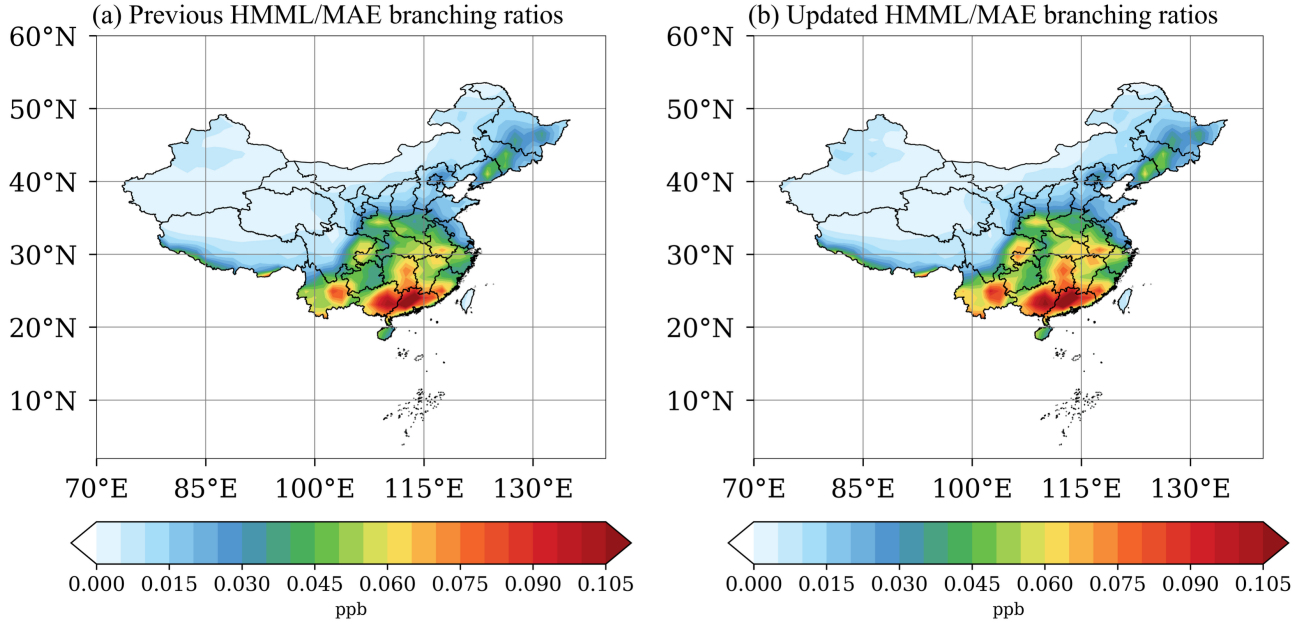

Figure R5: Comparison of annual mean surface concentrations of combined HMML and MAE (HMML + MAE) over China, averaged over the five simulation years (2000, 2006, 2012, 2016, and 2019) (unit: ppb), corresponding to the original Figure S3 in the Supplement. Panel (a) shows results obtained with the branching ratios adopted in the initially submitted implementation, in which MPAN + OH produced HMML and MAE with molar branching ratios of 0.57 and 0.21, respectively. Panel (b) shows results obtained with the revised branching ratios constrained by Nguyen et al. (2015), in which MPAN + OH produces HMML and MAE with molar branching ratios of 0.75 and 0.02, respectively.

Lines 168−170:

Methacrolein (MACR), the precursor of MPAN in the high-NOx pathway, is formed following the default MOZART-TS2 mechanism. The reaction of MPAN with OH yields HMML and MAE, with molar branching ratios of 0.75 and 0.02, respectively, based on the experimental results reported by Nguyen et al. (2015) (Table S2).

Comment#7: Line 146-147: The removal of the isoprene SOA formation in the VBS can potentially eliminate important non-epoxides contributions to isoprene SOA such as the multifunctional organic peroxides (low NOx) and organic nitrates (high NOx). Could authors give a proper account of this limitation?

Response: We thank the reviewer for this helpful comment. We agree that removing the OH-initiated ISOA formation from the default VBS scheme may affect the representation of non-epoxide ISOA pathways. In the revised manuscript, we have clarified the rationale and scope of this treatment. Specifically, the OH-initiated isoprene oxidation pathway in the VBS scheme was removed to avoid double counting between the default lumped VBS representation of ISOA and the explicitly represented epoxide-derived ISOA pathways. We have also added text clarifying that this treatment focuses the updated mechanism on epoxide-derived ISOA formation, although potential non-epoxide ISOA contributions originally included implicitly in the VBS scheme may not be explicitly resolved. In Sect. 4, we further note this as one of the uncertainties associated with the adopted chemical framework, together with other assumptions in the epoxide reactive uptake parameterization. These revisions have been incorporated in Sect. 2.1.2 (lines 172−176) and Sect. 4 (lines 672−675).

Lines 172−176:

To avoid double-counting between the default lumped VBS representation of ISOA and the explicitly represented epoxide-derived ISOA pathways, the OH-initiated isoprene oxidation pathway in the VBS scheme is removed (see Sect. 2.1.1). This treatment focuses the updated mechanism on epoxide-derived ISOA formation, although potential non-epoxide ISOA contributions originally included implicitly in the VBS scheme may not be explicitly resolved.

Lines 672−675:

Finally, the removal of ISOA formation from the VBS scheme may also remove important non-epoxide contributions to ISOA that were previously represented implicitly, such as multifunctional organic peroxides under low-NOx conditions and organic nitrates under high-NOx conditions (Paulot et al., 2009a; Schwantes et al., 2019).

Comment#8: Line 178-184: kaq is supposed to represent the sum of all particle-phase reactions that consume IEPOX. The reaction rate constant for nucleophilic reaction of IEPOX with water forming 2-methyltetrols is missing. kH+[H+] appears to be the acid-catalyzed isomerization reaction of IEPOX that forms diols and triols, but this pathway is excluded in the current representation. The unit for the third-order reaction rate constant knuc for sulfate and nitrate is incorrect. It appears to be second-order reaction. Please clarify and correct.

Response: We thank the reviewer for this helpful comment. As described in our response to the second part of Comment#2, we have replaced the initially submitted parallel-sink treatment with a relative-rate branching framework. In the revised manuscript, $k_{aq,total}$ is defined as the total pseudo-first-order aqueous-phase reaction rate constant that represents the sum of the particle-phase reaction channels consuming each epoxide precursor, including IEPOX, HMML, and MAE:

$$k_{aq,total} = k_{H^+}[H^+] + k_{nuc}([SO_4^{2-}] + [NO_3^-])[H^+] + k_{HSO_4^-}[HSO_4^-]$$

In this formulation, the first term represents acid-catalyzed ring opening followed by H_2O-mediated nucleophilic addition, leading primarily to methyltetrol-like products. We have revised the text to clarify that this term represents the H_2O-

mediated nucleophilic addition product channel and that this pathway is not missing or excluded in the revised representation. The second term represents acid-catalyzed ring opening followed by nucleophilic addition of sulfate and nitrate ions, leading to organosulfates and organonitrates. The third term represents concerted protonation and nucleophilic addition by bisulfate, leading to organosulfates. For each epoxide precursor, $k_{aq,total}$ is used to calculate the reactive uptake coefficient and the total uptake flux. The subsequent product allocation follows the relative-rate branching treatment described in our response to the second part of Comment#2.

We also standardized the notation and units for k_{nuc}. The apparent inconsistency arose from whether the acidity term was written as proton activity or proton concentration. In the revised manuscript, we use the concentration-based form consistently, $k_{nuc}([SO_4^{2-}] + [NO_3^-])[H^+]$, where $([SO_4^{2-}] + [NO_3^-])$ and $[H^+]$ are expressed in molar units. Therefore, k_{nuc} has units of $M^{-2}\,s^{-1}$, so that the full term has units of s^{-1}. These revisions have been incorporated into Sect. 2.1.2 of the revised manuscript (lines 196–242).

Comment#9: Line 196-197: Please be noted that 2-MT and 2-MGA are semi-volatiles that can partition into the gas phase. Regional models such as WFR-Chem (Shrivastava et al.,2022) and CMAQ (Pye et al., 2018) already accounted for gas/particle partitioning of 2-MT. This presents an opportunity for future improvements in global models.

Shrivastava, Manish, Quazi Z. Rasool, Bin Zhao, et al. "Tight Coupling of Surface and In-Plant Biochemistry and Convection Governs Key Fine Particulate Components over the Amazon Rainforest." ACS Earth and Space Chemistry 6, no. 2 (2022): 380–90. https://doi.org/10.1021/acsearthspacechem.1c00356.

Pye, Havala O. T., Andreas Zuend, Juliane L. Fry, et al. "Coupling of Organic and Inorganic Aerosol Systems and the Effect on Gas–Particle Partitioning in the Southeastern US." Atmospheric Chemistry and Physics 18, no. 1 (2018): 357–70. https://doi.org/10.5194/acp-18-357-2018.

Response: We thank the reviewer for pointing this out. We agree that treating epoxide-derived SOA products as non-volatile is a simplifying assumption, particularly because products such as 2-MT and 2-MGA may exhibit partial volatility and partition into the gas phase. In the revised manuscript, we have expanded the limitation discussion in Sect. 4 to clarify this uncertainty. Specifically, we now state that the assumption of 100% SOA yield from epoxide reactive uptake and the treatment of epoxide-derived SOA as non-volatile are consistent with previous global modeling studies of isoprene-derived SOA (Marais et al., 2016; Jo et al., 2019, 2021), but may affect the absolute ISOA burden and its sensitivity to heterogeneous reaction conditions.

We further note that existing gas–particle partitioning treatments for 2-MT in regional models provide a useful direction for future improvements in global models. We also clarify that lower effective yields or partial volatility, especially for products such as 2-MT and 2-MGA, could reduce simulated ISOA concentrations and their sensitivity to sulfate, aerosol liquid water, and acidity. This added discussion has been incorporated in Sect. 4 (lines 667−672).

Lines 667−672:

The assumptions of 100% ISOA yield from epoxide reactive uptake and non-volatile epoxide-derived ISOA introduce additional uncertainty, although they are consistent with previous global ISOA modeling studies (Marais et al., 2016; Jo et al., 2019, 2021). Lower effective yields or partial volatility, especially for products such as 2-MT and 2-MGA, could reduce simulated ISOA concentrations and their sensitivity to sulfate, aerosol liquid water, and acidity. Consistent with this need, gas–particle partitioning treatments for 2-MT in regional models suggest a useful direction for future improvement in global models (Pye et al., 2018; Shrivastava et al., 2022).

Comment#10: Lines 304-308: There is another ISOA peak in April but it coincided with low isoprene emissions. I am just curious if the authors have any thoughts on why this occurred? Also, the OH z-score seems to be missing in Figure 4b.

Response: We thank the reviewer for this helpful comment. We agree that the early warm-season ISOA enhancement deserves further clarification. In the revised Fig. 4(a), this feature appears as an early warm-season ISOA enhancement from April to May, before the summer maximum of biogenic isoprene emissions, and therefore cannot be explained by isoprene emissions alone.

We have revised the text to clarify that this early warm-season enhancement likely reflects the combined influence of several factors. During the transition from spring to early summer, biogenic isoprene emissions have already increased substantially from their winter levels, although they have not yet reached their annual maximum. At the same time, the rising standardized OH signal suggests strengthening oxidation capacity, which can promote the formation of isoprene oxidation products and epoxide precursors. Although the standardized sulfate and aerosol liquid water anomalies become lower during this period, they have not yet reached their most negative summer anomalies, so the multiphase reaction environment has not yet reached its least favorable summer state. Therefore, the April–May enhancement is interpreted as reflecting the combined effects of increasing precursor supply, enhanced oxidation capacity, and still available multiphase reaction conditions, rather than the dominance of a single factor.

We also thank the reviewer for pointing out that the OH z-score was missing from Fig. 4(b). The standardized seasonal cycle of OH was unintentionally omitted in the previous version. We have now added the OH z-score to Fig. 4(b), updated the legend, and revised the corresponding discussion in Sect. 3.2 (lines 406−411).

Lines 406−411:

The early warm-season ISOA enhancement from April to May further illustrates this combined-control behavior, but with a different balance among the controlling factors. It occurs before the annual maximum of isoprene emissions and during the rising phase of the standardized seasonal OH signal, but at a time when biogenic isoprene emissions have already increased substantially from spring, OH oxidation capacity is strengthening, and the multiphase reaction environment has not yet

reached its least favorable summer state. Thus, the May enhancement likely reflects the combined influence of increasing precursor supply, enhanced oxidation, and still favorable multiphase conditions, rather than the dominance of a single factor.

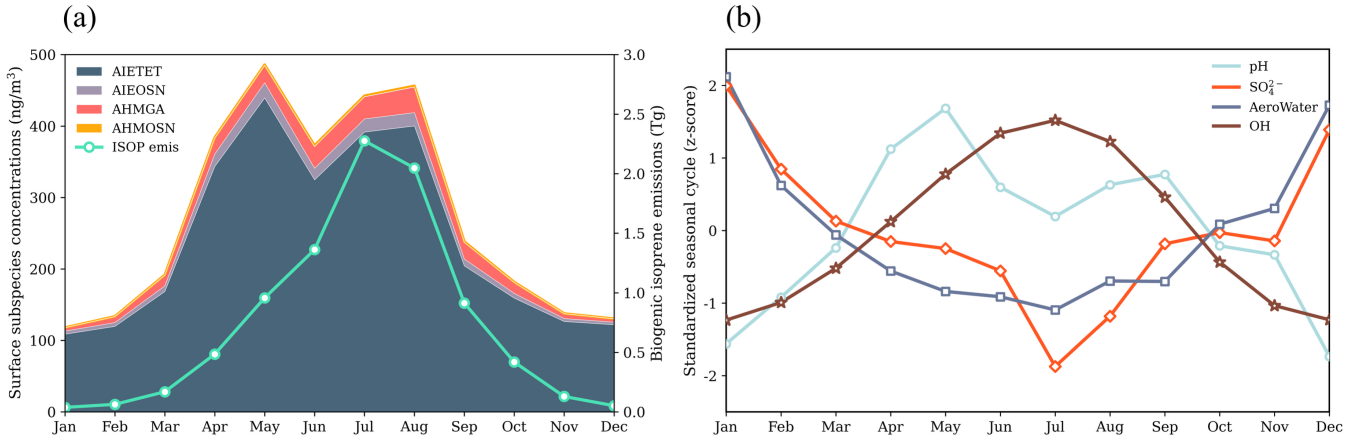

Figure 4: (a) Monthly variations of surface isoprene-derived secondary organic aerosol (ISOA) subspecies (left y axis; unit: ng m^{-3}) and biogenic isoprene emissions (ISOP emis; right y axis; unit: Tg) in China, based on the climatological monthly means averaged over the five simulation years (2000, 2006, 2012, 2016, and 2019). (b) Standardized monthly variations of background chemical and aerosol variables relevant to ISOA formation, including surface aerosol pH, surface sulfate (SO_4^{2-}) concentrations, surface aerosol liquid water (AeroWater) concentrations, and surface hydroxyl radical (OH) concentrations in China, based on the climatological monthly means averaged over the five simulation years.

Comment#11: Lines 335-337 (and Figure 5b): The surface area is the same and the epoxides mean speed is in the same ballpark. The only way khet_HMML+MAE and khet_IEPOX can differ by be a factor of 10 has to be due to the calculated coefficient γ. Therefore, I don't understand how the current model with HMML/MAE and IEPOX sharing the same parameters can lead to such different γ values. This relates back to my major comment 2. Please clarify if I missed something.

Response: We thank the reviewer for pointing this out. We agree that our previous wording could have led to ambiguity regarding the quantity shown in Fig. 5(b). The quantity shown in Fig. 5(b) is not the heterogeneous reaction rate coefficient k_{het} or the reactive uptake coefficient γ. Rather, it is the particle-phase ISOA production rate diagnosed from tagged heterogeneous reactions in the model. Therefore, the ratio shown in Fig. 5(b) reflects the formation rates of epoxide-derived ISOA products, rather than the ratio of khet or γ values for HMML/MAE and IEPOX. Specifically, the IEPOX-derived production rate is diagnosed by summing the tagged formation rates of IEPOX-derived particle-phase products, whereas the HMML/MAE-derived production rate is diagnosed in the same way from HMML/MAE-derived particle-phase products. Thus, these diagnosed production rates depend not only on the reactive uptake process, but also on the gas-phase precursor concentrations available for heterogeneous uptake. Under the current parameterization, HMML/MAE and IEPOX share the same uptake-related parameters, and therefore the model does not imply an order-of-magnitude difference in γ or k_{het} caused by different kinetic parameters. Instead, the lower particle-phase production rate of the HMML/MAE pathway mainly reflects the lower availability of HMML+MAE relative to IEPOX. To avoid this ambiguity, we have revised the text and figure description to explicitly refer to "particle-phase production rates diagnosed from tagged heterogeneous reactions"

rather than heterogeneous reaction rate coefficients. We also clarified that Fig. 5(b) is used to compare pathway-specific ISOA production rates, while Fig. 5(a) shows the corresponding gas-phase precursor ratio. These revisions have been incorporated in Sect. 3.2 (lines 444−450) and the caption of Fig. 5.

Lines 444−450:

To interpret this feature, we further compare the gas-phase precursors and particle-phase production rates diagnosed from the tagged heterogeneous reactions for the two pathways. The ratio of the gas-phase epoxide precursors HMML + MAE to IEPOX shows only a modest seasonal variation and generally remains within about 0.074 to 0.10 throughout the year (Fig. 5(a)). The ratio of tagged particle-phase ISOA production rates, $P_{HMML+MAE}/P_{IEPOX}$, exhibits a similar seasonal pattern, with an annual mean of about 0.10 (Fig. 5(b)). These results indicate that neither the HMML+MAE-to-IEPOX precursor ratio nor the corresponding tagged particle-phase ISOA production-rate ratio shows a comparably strong increase in September.

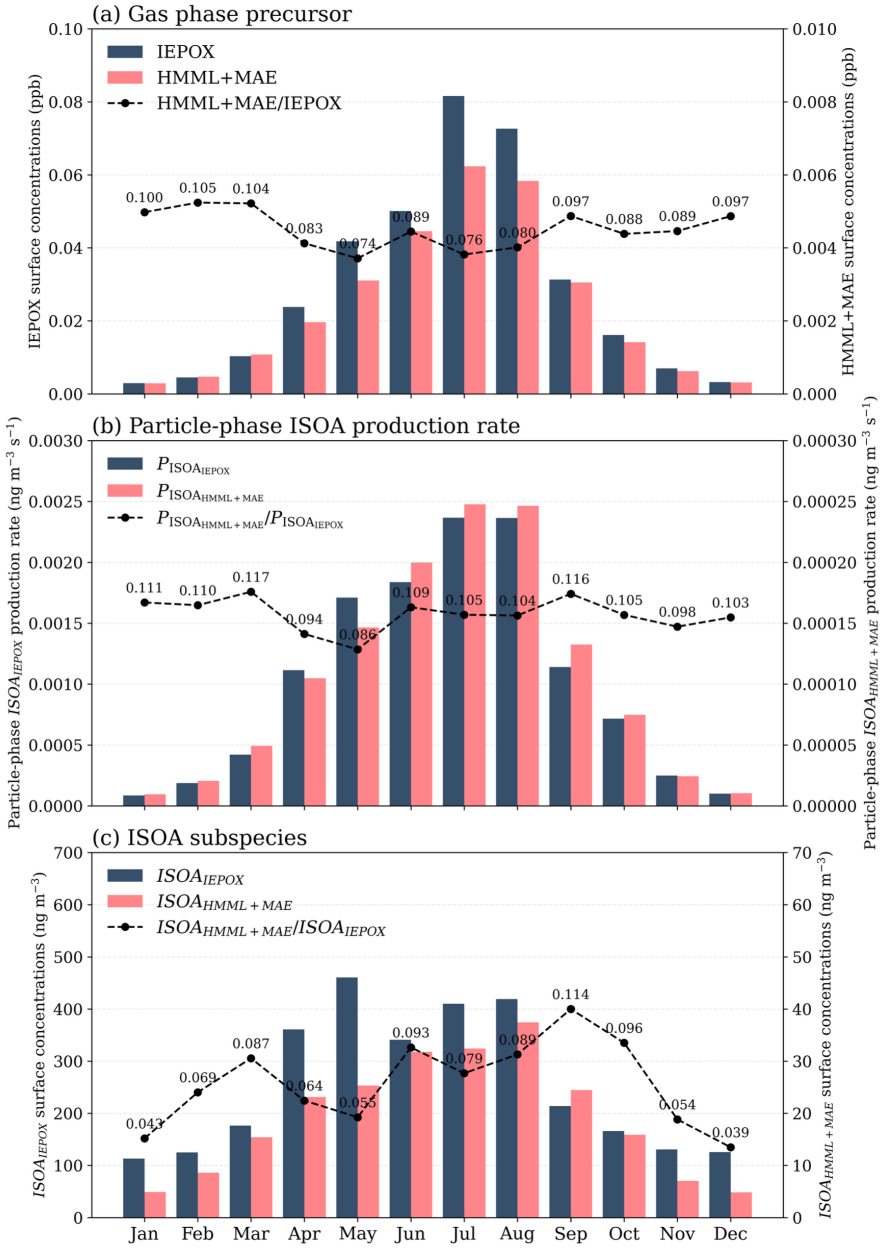

Figure 5: Monthly variations of IEPOX-related and HMML+MAE-related gas-phase precursors, particle-phase production rates, and ISOA concentrations in China, based on the climatological monthly means averaged over the five simulation years (2000, 2006, 2012, 2016, and 2019). (a) Surface concentrations of isoprene epoxydiols (IEPOX; dark-blue bars; left y axis; unit: ppb) and hydroxymethyl-methyl-α-lactone plus methacrylic acid epoxide (HMML + MAE; pink bars; right y axis; unit: ppb). (b) Particle-phase ISOA production rates diagnosed from tagged heterogeneous reactions for the IEPOX pathway ($P_{ISOA_{IEPOX}}$; dark-blue bars; left y axis; unit: ng m^{-3} s^{-1}) and the HMML+MAE pathway ($P_{ISOA_{HMML+MAE}}$; pink bars; right y axis; unit: ng m^{-3} s^{-1}). (c) Surface concentrations of ISOA derived from IEPOX ($ISOA_{IEPOX}$; dark-blue bars; left y axis; unit: ng m^{-3}) and ISOA derived from HMML and MAE ($ISOA_{HMML+MAE}$; pink bars; right y axis; unit: ng m^{-3}). In each panel, the black dashed line denotes the ratio of the HMML+MAE-related quantity to the corresponding IEPOX-related quantity, with monthly ratio values labeled above the markers.